New insights into the Formation of Complex Crater Rims: Structural Uplift, Ejecta Thickness and Transient Crater measurements of Complex Lunar Mare Craters. T. Krüger[1], T. Kenkmann[1], [1]Institut für Geo- und Umweltnaturwissenschaften, Albert-Ludwigs-Universität Freiburg, Albertstrasse 23-B, 79104 Freiburg, Germany (tim.krueger@geologie.uni-freiburg.de).

Introduction: Most complex impact craters on silicate bodies throughout the Solar System exhibit elevated crater rims similar to the elevated crater rims of simple craters. The final elevation of crater rims is due to the deposition of ejecta on uplifted bedrock of the paleosurface and is largest at the rim crest of the crater. Crater im uplift pinches out after 1.3 – 1.7 crater radii [1]. For simple craters the elevated crater rim is due to two well understood factors:

(1) Ballistically emplaced coherent proximal ejecta material at the transient cavity rim. A gradational transition from autochthonous bedrock to allochthonous ejecta exists in weakly modified simple craters in which the hinge zone of the overturned flap is preserved.

(2) Structural uplift of the pre-impact surface in the proximity of the transient cavity [1,2]. This uplift is created by horizontal shortening and can be accommodated by either a pervasive thickening of the target rocks, by reverse faulting, or the emplacement of interthrust wedges. In addition to shortening the injection of dike material into the cavity walls occurs [1-3].

Both factors equally contribute to the elevation of simple crater rims. Simple and complex impact craters show fundamental differences in their morphology and structure [1,4]. The spatial distance between the morphological crater rim of a complex crater and the edge of the transient cavity primarily depends on the impact energy and gravity. A consequence of the foregoing is that the ejecta thickness at the final crater rim of complex craters is usually less than the thickness at the rim of simple craters and may not contribute as significantly to the rim elevation as for simple craters. Dike injection of the underlying target has probably also a minor impact on the final complex crater rim. Thus, it cannot account for the observed elevation because the injection length of several kilometers is unlikely. We selected the pristine lunar mare craters Bessel (16 km), Euler (28 km), Kepler (32 km), Harpalus (39 km) and Bürg (41 km) since they show a range of different final crater diameters and all were formed in a uniform basaltic target. The selected craters show layered formation in their walls, originated from episodic flooding with basaltic magma, which filled the lunar Maria [5,6]. We reconstructed the transient crater cavity of these craters and additionally for 6 other craters, Aristachus (40 km), King (76 km), Copernicus (93 km), Tycho (95 km), Theophilus (100 km) and Pythagoras (130 km) with a geometric reconstruction model.

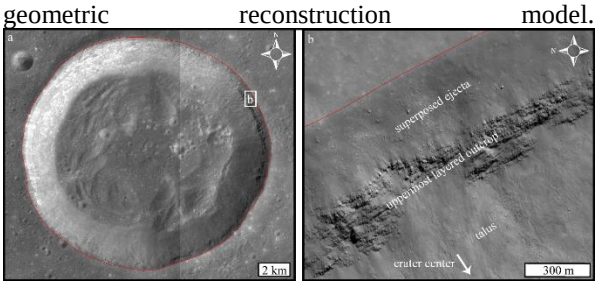

Fig.1: Layerd formation found in complex lunar Maria craters. (a) shows the 16 km crater Bessel with outcrops nearly throughout the complete crater wall. (b) part of an outcrop in greater resolution. This outcrop consists of several layers with a combined thickness of ~ 200 m.

Data: For our investigations we used high-resolution LROC-NAC, SELENE-TC-Ortho and LROC-WAC images combined with SELENE and WAC-GLD100 digital elevation models [7, 8, 9].

Methods: The elevation of the paleosurface *P* was determined by linear interpolation between two adverse points (a) situated beyond the continuous ejecta blanket. The linear goes through the crater center and the boundary between the uppermost exposed layer and the superposed ejecta. The elevation of the paleosurface *P* was calculated for each point at this boundary. Using new, more precise data, the ejecta thickness E_T was determined at each point. In a next step, using the exact spatial location of the layered outcrops, the structural uplift S_U of the exposed layer was calculated for each point (Fig. 2). The newly developed geometric reconstruction model (GRM) was used to calculate the dimension of the transient crater radius R_T; results of the model are compared to literature data [10,11]. We assumed that the terraced blocks are displaced along normal faults. During and after the collapse of the complex crater, the terraces were superposed by ejecta and talus material (Fig.3). Terrace are delimited by faults that have assumed dip angles (γ) of 60° [12], whereas the mean slope angle (α) is ~ 30° [1], close to the angle of respose for the scarps.

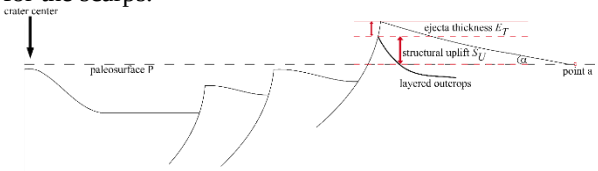

Fig.2: Schematic cross section of a complex crater rim and geometric relations for the calculation of ejecta thickness and structural uplift.

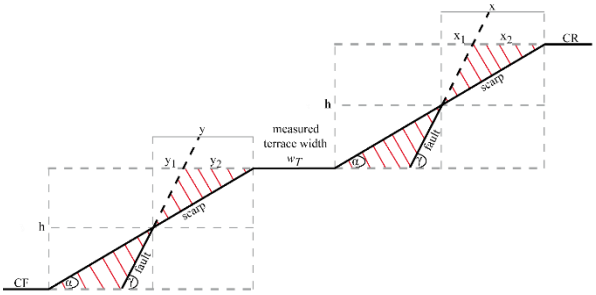

Fig.3: Geometric reconstruction model (GRM) to calculate the transient crater cavity of lunar complex craters. CF refers to crater floor and CR to crater rim. Red lines represent removed parts of the terrace and equivolumetric talus material covering part of the terraces.

Results: The average measured thickness of structural uplift and ejecta are summarized in Table 1. The measured ejecta thickness E_T reveals 29.4 % ± 11.2 %, whereas the mean structural uplift S_U amounts to 70.6 % ± 11.2 % of the rim elevation. The structural uplift S_U and ejecta thickness E_T at the final crater rim increase with increasing size of the crater. However, the ratio of both remains constant within the limit of error. The radii of the transient crater cavities R_T were calculated with our geometric reconstruction model (GRM) and the results are shown in Table 2. For comparison transient crater cavities calculated from literature are listed as well [10,11]. The ratio of the final crater R_F to the transient crater R_T ranges between 1.21 and 1.48, using our geometric model.

Table 1: Minimum structural uplift and maximum ejecta thickness data determined in this study.

	Bessel	Euler	Kepler	Harpalus	Bürg
R_F [m]	7896.1 ± 199.8	13526.7 ± 426.6	15042.6 ± 266.6	19883.7 ± 286.2	22395.8 ± 2852.2
P [m]	-2560.9 ± 32.1	-1308.1 ± 61.0	-1027.1 ± 35.8	-2496.4 ± 77.0	-1899.9 ± 126.9
S_U [m]	443.1 ± 115.7	533.4 ± 154.1	551.2 ± 200.6	706.2 ± 133.3	846.7 ± 220.6
E_T [m]	173.1 ± 51.7	220.3 ± 113.2	251.6 ± 75.9	251.4 ± 73.7	298.3 ± 79.9

Table 2: Transient crater radii determined in this study. [1]For Bessel crater we used the Debris-slide reconstruction model from [10].

	R_T [10] [m]	R_T [11] [m]	R_T (GRM) [m]	R_F/R_T for GRM
Bessel	7776.6[1]	-	-	1.02
Euler	12500.6	13437.0	9888.4 ± 1190.9	1.39 ± 0.01
Kepler	13997.6	15188.9	10084.6 ± 1296.5	1.48 ± 0.01
Harpalus	17346.4	19163.2	14304.8 ± 1295.3	1.39 ±0.03
Aristachus	17548.4	19405.0	14606.9 ± 931.2	1.38 ±0.02
Bürg	19190.8	21380.3	16347.3 ± 812.4	1.37 ± 0.06
King	30459.3	35269.7	28356.1 ± 117.8	1.36 ± 0.01
Copernicus	35789.9	42004.1	34534.3 ± 287.12	1.35 ± 0.04
Tycho	36329.8	42691.2	35026.3 ± 67.6	1.35 ± 0.01
Theophilius	38119.5	44974.5	39536.7 ± 253.9	1.27 ± 0.05
Pythagoras	47778.2	57443.6	54126.6 ± 167.9	1.21 ± 0.04

Discussion and Conclusion: Early studies and models show that the elevation of the crater rim is equally distributed between structural uplift and superposed ejecta deposits [1, 2]. Whereas this might be true for simple craters, our results show, that for complex craters this correlation changes to a S_U of 70.6 % ± 11.2 % and a E_T of 29.4 % ± 11.2 %. A reduction of the ejecta thickness by erosion or impact gardening is unlikely as the craters appear fresh. The recent study by [13] shows comparable results with S_U of ~ 80 % and E_T of ~ 20 %. The injection of impact melt or breccia into the bedrock [13] seems unlikely at distances between 1.21 and 1.48 R_T. Therefore, we propose that reverse faulting, beginning in the excavation stage of crater formation, is responsible for the additional structural uplift of the crater rim. This would imply that the final crater morphology would be pre-determined during the excavation stage.The results of this work are consistent with the work of other authors [1,13,14,15].

Acknowledgements: This project was financed by the German Research Foundation DFG, grant KE 732/21-1.

References: [1] Melosh H.J. (1989*) Oxford monographs on geology and geophysics, 11,* Impact cratering: a geologic process [2] Shoemaker, E. M. (1963), *In* Middlehurts, B. M., and Kuiper, G. P. (eds.) *The Solar System, 4*, 301-336. [3] Poelchau M.H. et al. (2009) *JGR, 114*, E01006. [4] Settle and Head (1977) *Icarus, 31*, 123 – 135. [5] Hiesinger H. et al. (2002) *GRL, 29.* [6] Enns A.C. (2013) *LPSC XLIV*, #2751. [7] Robinson M.S. et al. (2009), *Space Science Reviews, 150*. [8] Haruyama J. et al. (2008), *Advances in Space Research, 42*. [9] Haruyama J. et al. (2006), *LPSC XXXVII*, #1132. [10] Croft S.K. (1985) *JGR, 90*, C828 – C842. [11] Holsapple K.A. (1993) *Annu. Rev. Earth Planet Sci, 21*, 333 – 373. [12] Nahm et al. (2013) *JGR, 118*, 190 – 205. [13] Sharpton, V. L. (2014) *JGR*, 119. [14] McGetchin, T. R. et al. (1973), *Earth Planet. Sci. Let., 20*, 226-236. [15] Sturm, S. et al. (2014), *LPSC XLV*, #1801.